A FEM-based model to study the behaviour of corroded RC beams shear repaired by NSM CFRP rods technique

Conference Paper · April 2015

CITATIONS
2

READS
70

4 authors:

Bélal Almassri
Palestine Polytechnic University
15 PUBLICATIONS **37** CITATIONS
SEE PROFILE

Joaquim A.O. Barros
University of Minho
473 PUBLICATIONS **3,730** CITATIONS
SEE PROFILE

Firas Al-Mahmoud
University of Lorraine
37 PUBLICATIONS **321** CITATIONS
SEE PROFILE

Raoul Francois
Institut National des Sciences Appliquées de …
149 PUBLICATIONS **2,857** CITATIONS
SEE PROFILE

Composite Structures 131 (2015) 731–741

Contents lists available at ScienceDirect

Composite Structures

journal homepage: www.elsevier.com/locate/compstruct

A FEM-based model to study the behaviour of corroded RC beams shear-repaired by NSM CFRP rods technique

Belal Almassri [a], Joaquim A.O. Barros [b], Firas Al Mahmoud [c,*], Raoul Francois [a]

[a] Université de Toulouse; UPS, INSA, LMDC (Laboratoire Matériaux et Durabilité des Constructions), Toulouse, France
[b] ISISE, Dep. Civil Eng., Minho University, Guimarães, Portugal
[c] Institut Jean Lamour, UMR 7198, CNRS, Université de Lorraine, Nancy, France

ARTICLE INFO

Article history:
Available online 19 June 2015

Keywords:
Corrosion
Repair
RC beams
NSM CFRP rods
FEM
Shear

ABSTRACT

This paper presents the main features of a finite element FE numerical model developed using the computer code FEMIX to predict the contribution of near-surface mounted (NSM) carbon-fibre-reinforced polymer (CFRP) rods to the shear repair of corroded reinforced concrete RC beams. In the RC beams repaired in shear with the NSM technique, the CFRP rods are placed inside grooves pre-cut into the concrete cover of the RC beam's lateral faces and are bonded to the concrete with high performance epoxy adhesive. Experimental and 3D numerical modelling results are presented here in terms of load–deflection curves and failure modes for 4 short corroded beams: two corroded beams (A1CL3-B and A1CL3-SB) and two control beams (A1T-B and A1T-SB), the beams noted B were repaired in bending only with NSM CFRP rods while those noted SB were repaired in both bending and shear with the NSM technique. The corrosion of the tensile steel bars and its effect on the shear capacity of the RC beams is discussed. Results show that the FE model is able to capture the main aspects of the experimental load–deflection curves of the RC beams. They also present the experimental failure modes and FE numerical modelling crack patterns, both of which gave similar results for non-shear repaired beams, which showed a diagonal tension mode of failure, and for shear-repaired beams, which failed due to a large flexural crack in the middle of the beams, along with the concrete crushing. Three-dimensional crack patterns were produced for shear-repaired beams in order to investigate the splitting cracks occurring at the middle of the beams and near the support.

1. Introduction

The deterioration of reinforced concrete (RC) structures is a serious issue for many nations, as it could put public safety in jeopardy and the escalating repair cost could directly burden the future economy [1]. The corrosion of steel reinforcement is still one of the major concerns as it may lead to significant reduction in terms of ultimate capacity and serviceability of RC structures [2,3]. Many studies have presented the effect of steel corrosion on the flexural behaviour of RC structures [4–7] but very few show the effect of corrosion on the shear capacity of such structures. Moreover, most of the available literature [8–10] studies the effect of corrosion on the shear behaviour of RC beams by using impressed current to induce corrosion of the steel bars. These accelerated systems do not represent the real state of corroded structures but very few studies have aimed to study naturally corroded structures. The studies of this type that exist were based on long-term natural corrosion systems [11,12] in which the RC beams were stored in a chloride environment under service loads.

Near surface mounting of CFRP rods is a promising strengthening technique to increase the shear resistance of RC beams that have some risk of collapsing in a brittle shear failure mode. Shear strengthening of RC beams by NSM CFRP rods consists of fixing the CFRP rods, by means of a high performance epoxy adhesive, into thin grooves cut onto the concrete cover of the RC beams' lateral faces. Several experiment-based studies have investigated the efficiency of using the NSM CFRP rods technique in the shear strengthening of RC beams [13–15]. Other studies have used NSM CFRP laminates (strips), instead of round bars, to study the effect of the NSM technique on the shear capacity of RC beams [16,17]. Nanni et al. [18] predicted the contribution of NSM systems to the shear resistance of RC beams but this prediction was based on the assumption that laminate debonding was the dominant mode of failure. The separation of the concrete cover containing the laminates is always more frequently reported in relevant

* Corresponding author.
E-mail address: firas.al-mahmoud@univ-lorraine.fr (F. Al Mahmoud).

http://dx.doi.org/10.1016/j.compstruct.2015.06.030
0263-8223/

studies [15,19]. Bianco et al. [20] have produced an analytical model that is able to predict the contribution of NSM CFRP laminates to shear strength on the basis of various possible modes of failure: debonding; concrete semi-conical tensile fracture; mixed shallow-semi-cone-plus-debonding; and strip tensile fracture.

The NSM technique to repair corroded RC beams has hardly been studied. Bending strengthening is mainly concerned and only a very recent paper [21] has studied the NSM effect on the experimental shear behaviour of corroded RC beams.

The available research shows that the predictive performance of computer programs based on the finite element method (FEM) for the non-linear analysis of RC structures failing in shear is closely related to the constitutive model used to simulate shear stress transfer in cracked concrete [22,23]. Suryanto et al. [23] mention the significant requirement that the shear stress–strain softening law for concrete should be taken into account in order to capture the real damage that occurs in concrete during the cracking process. There are some studies available [24–26] that use FE modelling programs to study the effect of applying the NSM technique to the shear strengthening of RC beams: a multi-directional fixed smeared crack model was implemented by Barros et al. [26] to simulate the CFRP strengthened RC beams failing in shear and flexure, and Barros et al. [19] investigated the effectiveness limitations of the NSM CFRP laminates technique in shear strengthening of RC beams using the FEMIX computer code and recorded the failure of concrete volume including the CFRP laminates.

There are no numerical modelling studies available that were performed to investigate the mechanical behaviour and failure modes of corroded RC beams repaired in shear with NSM CFRP rods. The present paper implements an FE model using the FEMIX computer code to study the performance of corroded short-span reinforced concrete beams repaired with the NSM FRP technique. Some of the beams were repaired in bending only and the others were repaired in bending and shear. All beams were tested experimentally in three-point loading up to failure. The FE model investigated the failure modes and the shear capacities for all RC beams, and the shear capacity of the short-span corroded beams repaired in shear and bending was compared to that of non-repaired similar beams.

2. Experimental programme

2.1. Experimental procedure

An experimental programme aimed at understanding the effects of steel corrosion on the structural behaviour of RC elements was started at LMDC (Laboratory of Materials and Durability of Constructions) in 1984. Many experimental studies have since been conducted on those beams to evaluate the development of corrosion cracking, to measure chloride content and to analyse changes in mechanical behaviour [27,28]. Details of the natural aggressive environment system can be found elsewhere [29].

The four (80 cm) RC beams studied in this paper were cut from two long beams. Two short corroded beams were obtained from a long corroded RC beam (A1CL3-R) and two control beams were taken from the long control (non-corroded) RC beam (A1T-R). The two full span length beams were repaired with one 6-mm-diameter CFRP rod in bending and tested in three point loading up to failure. More details of the long beams can be found elsewhere [30]. Two short RC beams, one corroded (A1CL3-SB) and one control (A1T-SB), were shear repaired with NSM CFRP rods while two others; one corroded (A1CL3-B) and one control (A1T-B) were kept repaired in bending only. The reinforcement layout of the full length beams and the four short beams is shown in Fig. 1.

2.2. Main experimental results

2.2.1. Corrosion results

After the tensile steel bars and steel stirrups had been extracted from the two corroded beams and cleaned with Clark's solution ANSI/ASTM G1-72, the diameter loss was calculated with a weight

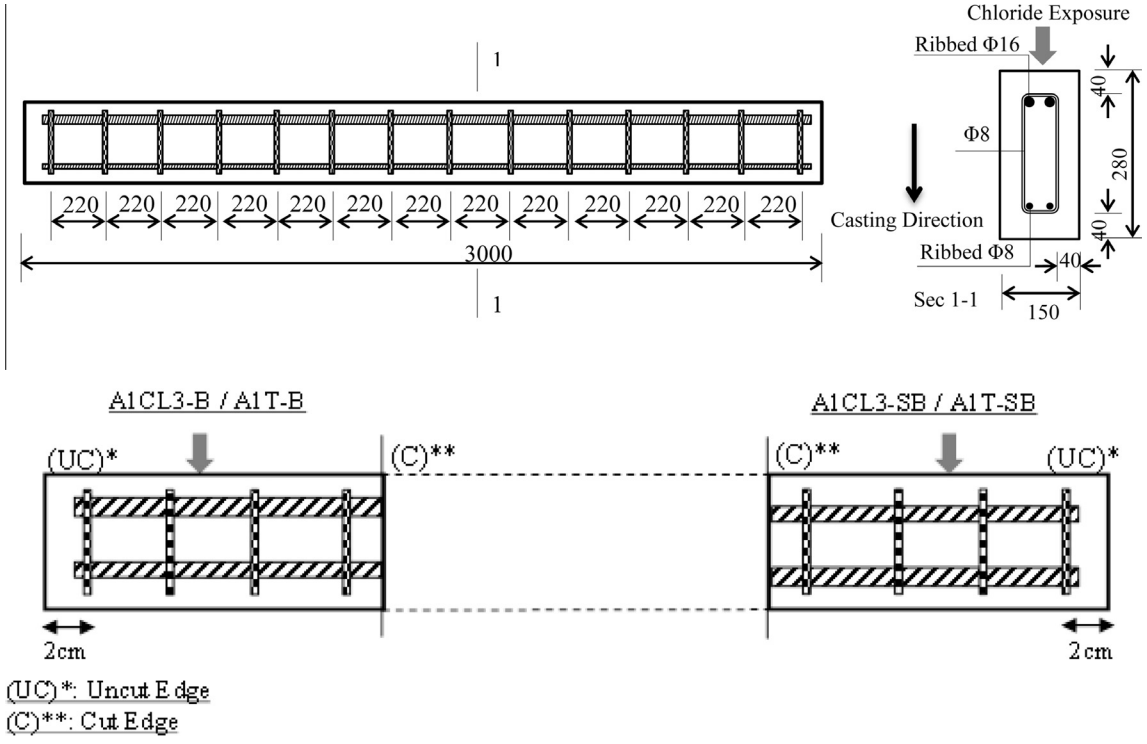

Fig. 1. Reinforcement layout all beams. Dimensions are in mm.

loss method because the high scatter in the corrosion shape did not allow it to be measured directly using a Vernier calliper. According to the corrosion pattern, short pieces of corroded steel bars were cut and weighed to measure the loss of mass due to corrosion. Fig. 2 shows that the maximum diameter loss found in the beam A1CL3-B was 18% while, for A1CL3-SB, it was 9%.

For the corroded beam A1CL3-R, the steel stirrups were numbered to indicate the part of the beam they came from and their position in that part (the first number representing the part of the beam and the second number being the number of the stirrup) as shown in Fig. 3, which also presents the stirrup numbers of the non-repaired corroded RC beam A2CL2-A studied by Dang et al. [31] that will be used here for comparison.

Fig. 4(a) shows the locations of corrosion in the steel stirrups and the diameter values for the corroded beam A1CL3-R. No corrosion was found at stirrups 1-1 and 1-2. The maximum diameter loss found in beam A1CL3-B was 63% at stirrup 1-4 (at the far edge of the diagonal shear crack) while the maximum loss in A1CL3-SB was 38% at stirrup 3-1. Fig. 4 also shows the corrosion map (% diameter loss) for corroded beam A2CL2-A. The maximum diameter loss found was 77% (1.84 mm) at the edge where the diagonal shear crack occurred.

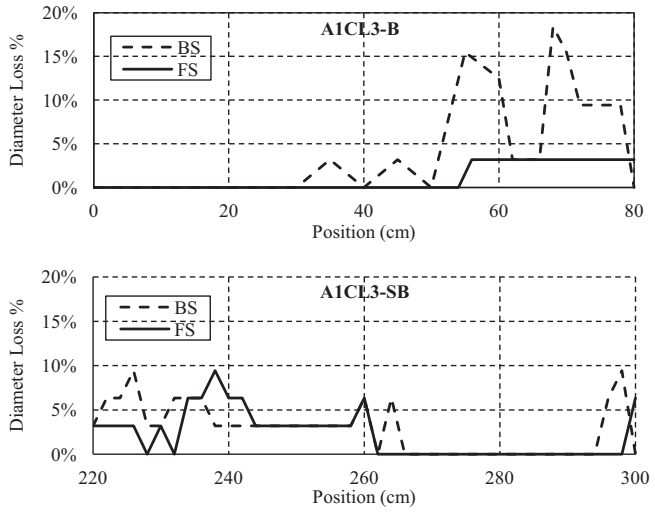

Fig. 2. Diameter loss percentages of longitudinal tensile steel bars from corroded beams.

2.2.2. Ultimate load capacity and modes of failure

The four RC beams tested were compared with two other beams: the corroded beam A2CL2-A and the control tested by Dang et al. [31]. Fig. 5 shows the load–deflection curves for all short beams tested experimentally. The shear strengthening increased the shear capacity of the control beams, while the shear strengthening response of the corroded beams depended on the pattern and the intensity of steel corrosion.

The difference in the yielding capacity of the shear-repaired control beam A1T-SB and the shear-repaired corroded beam A1CL3-SB is associated with the 12% loss in cross section found at the middle of the corroded beam A1CL3-SB (the load-induced crack occurs at mid-span), while the decrease in the yielding capacity for non-shear repaired corroded beam A2CL2-A in comparison with non-shear repaired beams (Control, A1T-B and A1CL3-B) is associated with the 10% loss in cross section found at the edge of the corroded beam A2CL2-A (the same edge as the diagonal shear crack) [31].

Experimental results also showed that shear strengthening with NSM CFRP rods changed the mode of failure from diagonal crack failure close to the support due to slipping of the tensile re-bars at anchorage (for non-shear-repaired beams A1T-B and A1CL3-B), to failure by a large flexural crack at mid span followed by concrete crushing (for shear-repaired beams A1T-SB and A1CL3-SB) as shown in Fig. 6.

It is also noteworthy that, for shear-repaired beams A1T-SB and A1CL3-SB, many splitting cracks occurred mid-way through the beam's width as shown in Fig. 7. These splitting cracks were easy to see at the bottom of the beam and at the beam edges near the supports. More details of the experimental programme for the short beams can be found elsewhere [21], together with the experimental results.

3. Numerical model

In this study, a multi-directional fixed smeared crack model was used to simulate the RC beams failing in shear. The most important aspect of this constitutive model is that it uses concrete fracture modes I & II by using a softening diagram in order to simulate the crack shear stress vs. crack shear sliding in the context of a smeared approach. The description of the formulation of the multi-directional fixed smeared crack model is restricted to the case of cracked concrete here. This model is described in greater detail elsewhere [19].

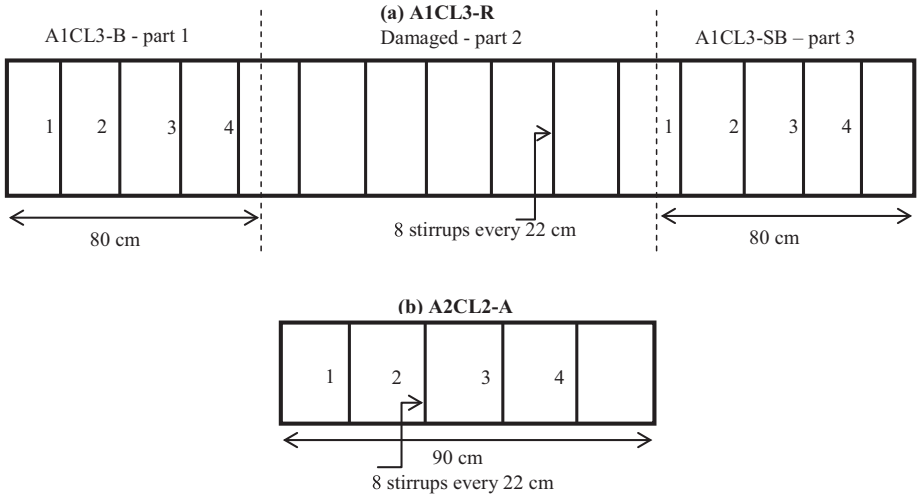

Fig. 3. Stirrups numbers of corroded beams (a) A1CL3-R (b) A2CL2-A.

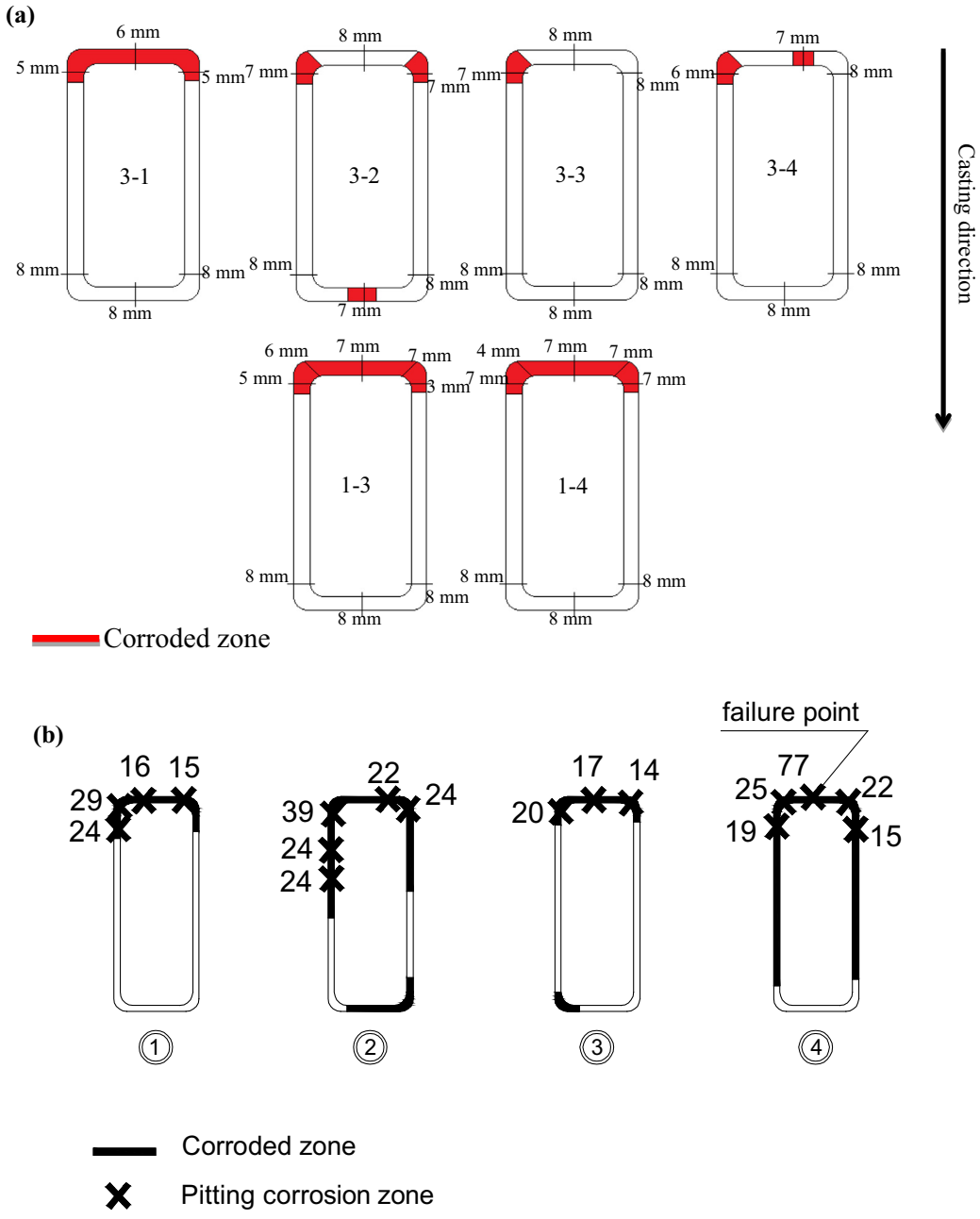

Fig. 4. Stirrup corrosion maps (a) diameter in mm for A1CL3-R (b) diameter loss % in A2CL2-A.

3.1. Concrete properties

Three-dimensional 20-node (quadratic) solid elements were used to simulate the concrete material in this numerical model. The concrete properties used are shown in Table 1.

3.1.1. Concrete fracture mode I: "tension softening of concrete"

The crack evolution in fracture mode I was simulated using a tri-linear tension softening or stiffening diagram as shown in Fig. 8. In structures controlled by flexural modes of failure, there would be no need to adopt a softening crack shear stress vs. crack shear strain relationship in the numerical model.

3.1.2. Concrete fracture mode II: "shear softening of concrete"

Suryanto et al. [23] showed that taking the shear softening law into account when modelling the shear stress transfer in cracked concrete was fundamental in order to better simulate the behaviour of engineered cement composite (ECC) beams failing in shear. Therefore, in this paper, a linear shear softening law (shown in Fig. 9) for modelling fracture mode II of cement based materials is used.

3.2. Steel properties

The steel reinforcement bars were implemented in this model as elastic–plastic behaviour. A Poisson's ratio of 0.3 was used and the elastic modulus and yield strength values of steel reinforcement bars and stirrups were as in Table 2 for both control and corroded steel bars. The post yielding hardening behaviour of control and corroded steel bars and steel stirrups was modelled as shown in Figs. 10 and 11 respectively. Corrosion did not modify the actual yield strength and hardly modified the actual ultimate strength [32,33] but it strongly decreased the ultimate elongation [34–37].

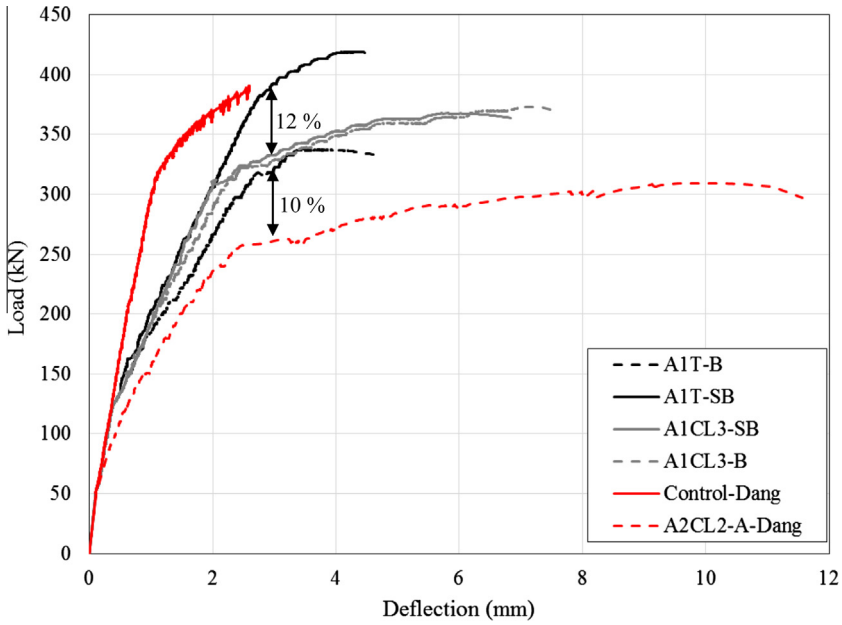

Fig. 5. Load–deflection curves for all beams.

Fig. 6. Experimental modes of failure for all tested beams.

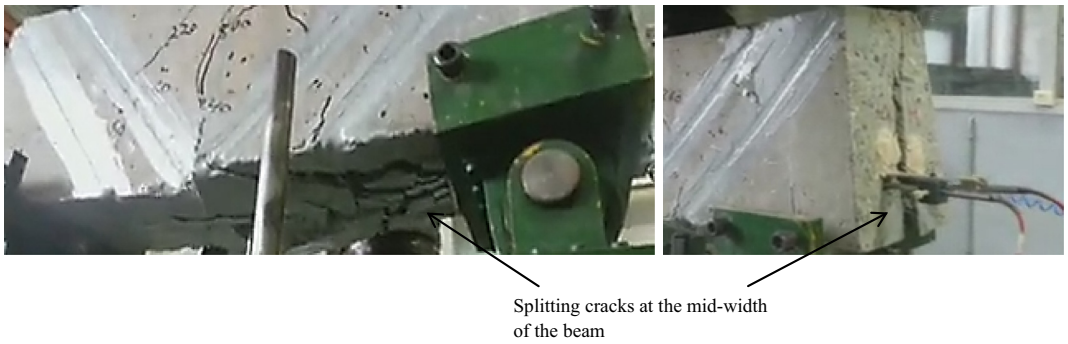

Fig. 7. Tensile steel bars slip occurred in non-shear repaired beams A1T-SB and A1CL3-SB.

Table 1
Concrete properties.

Poisson's ratio	$v_c = 0.20$
Initial Young's modulus	$E_c = 30000$ N/mm^2
Compressive strength	$f_c = 60$ N/mm^2
Tri-linear tensile-softening diagram	$f_{ct} = 4.5$ N/mm^2, $G_f^I = 0.05$ N/mm $\xi_1 = 0.005$, $\alpha_1 = 0.5$, $\xi_2 = 0.3$, $\alpha_2 = 0.2$
Parameter defining the mode I fracture energy available to the new crack	$P_2 = 1$
Shear softening parameters	$\tau_{t,p}^{cr} = 3$ N/mm^2, $G_{fs} = 0.1$ N/mm, $\beta = 0.1$
Threshold angle	$\alpha_{th} = 30°$
Maximum number of cracks per integration point	2

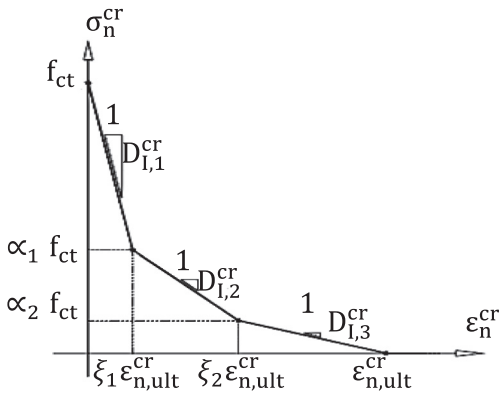

Fig. 8. RC fracture mode I "tri-linear tension softening diagram".

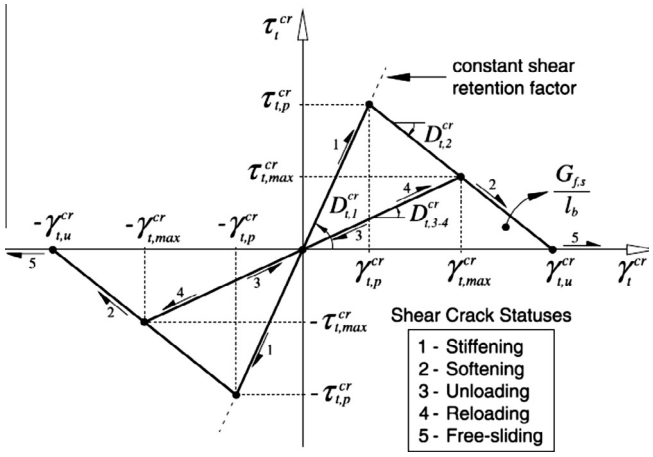

Fig. 9. RC fracture mode II "linear shear softening diagram".

3.3. CFRP properties

To model the NSM CFRP rods, a linear elastic stress–strain relationship was implemented. Table 3 presents the values used in the constitutive model for CFRP rods according to the manufacturer's specifications.

3.4. Modelling of RC beams bending and shear-repaired with NSM CFRP rods (A1CL3-SB and A1T-SB)

The main objective of this part of the work was to create a reliable numerical model that could simulate and predict the global behaviour (load–deflection curves and modes of failure) of two RC beams repaired in shear with NSM CFRP rods (corroded beam A1CL3-SB and control beam A1T-SB). Both beams had already been repaired with NSM CFRP rod in bending as they were taken from full length beams A1CL3-R and A1T-R, two long beams that had already been tested [30]. To simulate the concrete in the beams, three-dimensional solid 20-node elements with 3×3 Gauss–Legendre integration were used. The steel bar and stirrup reinforcements, and the CFRP rods, were simulated using 3-node quadratic three-dimensional embedded cable elements with two Gauss–Legendre integration points. The epoxy adhesive material was not represented in this model as a previous study [24] had shown that the epoxy adhesive had a negligible effect on the global behaviour of the RC beams. Figs. 12 and 13 show the geometry, elements mesh, loading and support configuration.

In order to avoid the distortion of elements that could occur as a result of the point load in the FE numerical model, an edge load was implemented in this model as shown in Fig. 13. Moreover, in all numerical models, the edge load was applied by direct displacement-control at the point located in the lower right corner of the mesh.

3.4.1. Modelling of corroded RC beam A1CL3-SB

In this numerical model, the diameter loss at the middle of the beam (6%) found in tensile steel bars of the corroded beam A1CL3-SB (see Fig. 2) was used as a constant residual re-bar cross section all along the RC beam. The reduced cross-sectional area at the mid-span point was used as the failure mode recorded experimentally for this beam was due to large crack at the middle of the beam.

3.5. Modelling of RC beams not shear-repaired with NSM CFRP rods (A1CL3-B, A1T-B and A2CL2-A)

One FEM model was implemented for the beams with NSM CFRP rods that were not repaired in shear. The model took account of the cross sectional area reduction due to steel corrosion for both tensile steel bars and steel stirrups at the failure location. The same numerical modelling properties of the fracture mode parameters for the concrete were used here and the FE model took two different constitutive steel models into account (one for corroded beams and one for control beams). Fig. 14 shows the geometry, element mesh, loading and support configuration for the three beams not shear-repaired with NSM CFRP rods A1CL3-B, A1T-B and A2CL2-A.

4. Numerical modelling results

4.1. Load–deflection curves and failure modes for RC beams not shear-repaired with NSM CFRP rods (A1CL3-B, A1T-B and A2CL2-A)

One FE model was used for beams A1CL3-B and A1T-B as no noteworthy steel corrosion (either in tensile steel bars or in steel stirrups) was found at the edge of the corroded beam A1CL3-B

Table 2
Average values of steel bars properties.

Specimen type	Young's modulus (GPa)	Yield strength (MPa)	Ultimate strength (MPa)	Ultimate strain
Non-corroded steel specimen	200	550	604	0.08
Corroded steel specimen	200	550	645	0.04

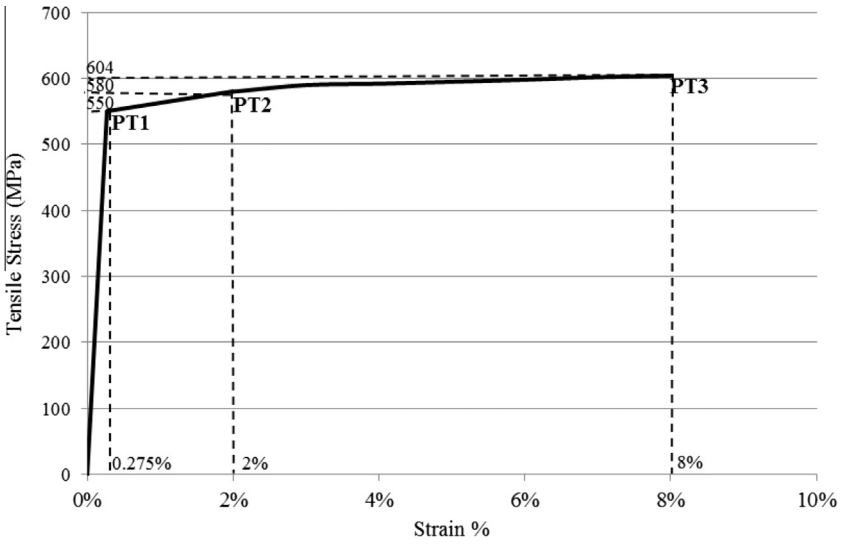

Fig. 10. Uniaxial constitutive model of non-corroded steel bars.

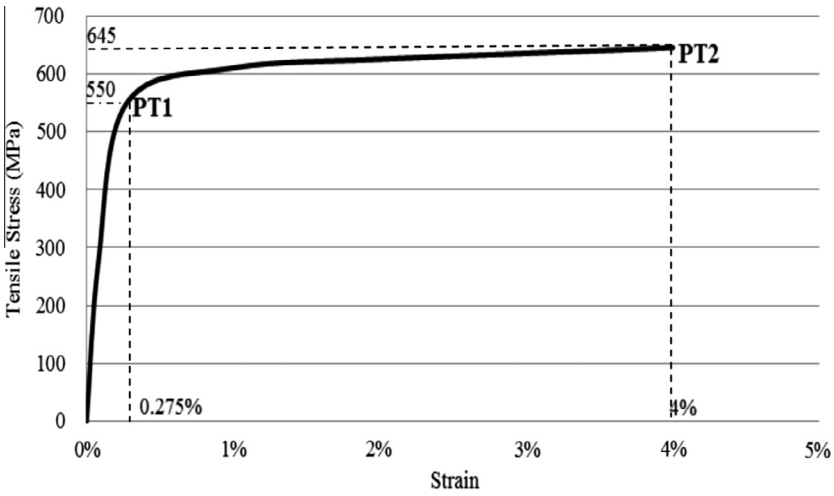

Fig. 11. Uniaxial constitutive model of corroded steel bars.

Table 3
CFRP rod characteristics.

Type of test	Ultimate strength (MPa)	Modulus of Elasticity (MPa)
Manufacturer's test	2300	150,000

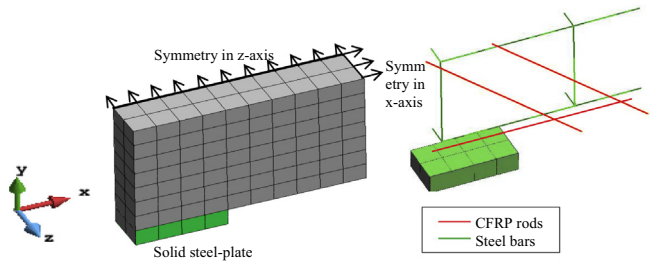

Fig. 12. The boundary conditions of the 3D model in an isometric plane in GiD-FEMIX.

(the same diagonal shear crack edge). The FE model was used again for the corroded beam A2CL2-A (tested experimentally by Dang et al. [31]) using the 10% loss of tensile steel bar cross section, due to corrosion, which was found at the edge of the beam (the same diagonal shear crack edge) as a constant residual re-bar cross section all along the RC beam. The diameter found for the steel stirrups at the failure point of the corroded beam A2CL2-A, which was 1.84 mm (77% of diameter loss shown in Fig. 4(b)), was used in this model as a constant residual cross section for all of the steel stirrups in the RC beam. For A2CL2-A modelling, the uniaxial constitutive law of corroded steel (shown in Fig. 11) was used. The load–deflection curves for the FE numerical model for the three non-shear-repaired beams A1CL3-B, A1T-B and A2CL2-A were drawn with the experimental load–deflection curves in Fig. 15.

Fig. 15 shows good agreement between FE numerical models and experimental results for the load–deflection behaviour. Although full numerical convergence was not obtained and capturing the post-yielding behaviour for RC beams failing in shear was difficult to achieve for this point since several new cracks formed and, at the same time, the old existing cracks changed their status. Fig. 15 also shows that considering the steel corrosion for both tensile steel bars and steel stirrups in the FE numerical models led to a

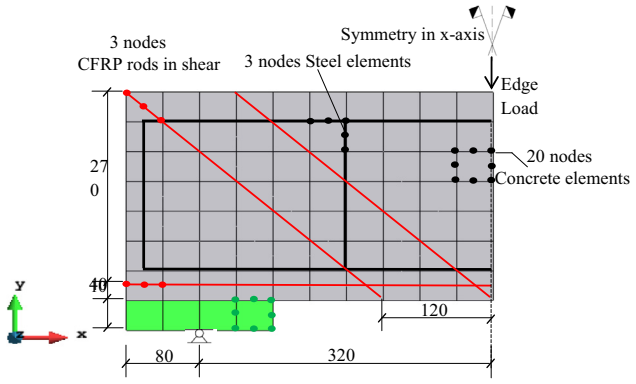

Fig. 13. Geometry in (mm), mesh, loading and support conditions in *x–y* plane for beams repaired in shear with NSM CFRP rods.

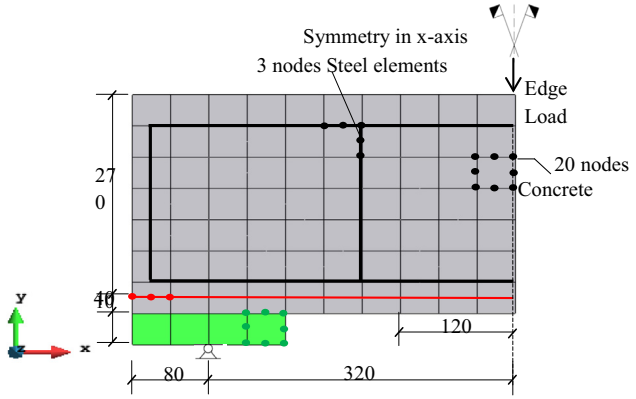

Fig. 14. Geometry in (mm), mesh, loading and support conditions in *x–y* plane for beams not shear-repaired with NSM CFRP rods.

reduction of 48 kN in the yielding-moment capacity of the corroded RC beam A2CL2-A (56 kN loss of yielding-moment capacity was found experimentally). The same yielding capacity was obtained for beams A1T-B and A1CL3-B as the corroded beam A1CL3-B had no corrosion at the edge where the shear failure occurred. The crack pattern of the non-shear-repaired beams was obtained using FEMIX code and it is presented in Fig. 16.

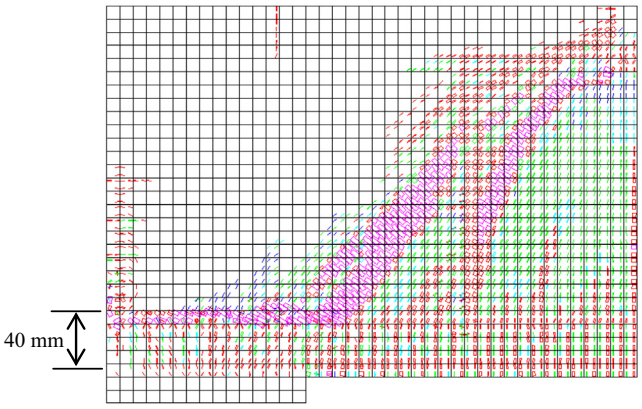

Fig. 16. FE crack pattern of the non-shear-repaired beams (in pink: crack completely open; in red: crack in the process of opening; in cyan: crack in the process of reopening; green: crack in the process of closing; in blue: closed crack). (For interpretation of the references to color in this figure legend, the reader is referred to the web version of this article.)

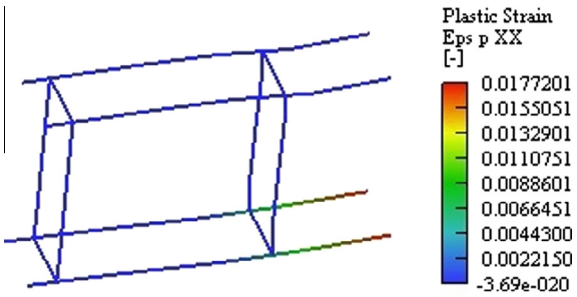

Fig. 17. Maximum strain values in the steel bars for the non-shear repaired beam A1CL3-B.

The open diagonal shear cracks shown in Fig. 16 present the modes of failure for both beams not shear-repaired with NSM obtained by the FE numerical model, which coincide with what was found experimentally (see Fig. 6). The diagonal cracks remained horizontal near the support at the location of the tensile steel bars (40 mm from the surface).

The numerical FE model showed that the maximum strain value reached in the tensile bars of the corroded beam A1CL3-B was 0.02 (shown in Fig. 17) which is still less than the 0.04 ultimate reduced

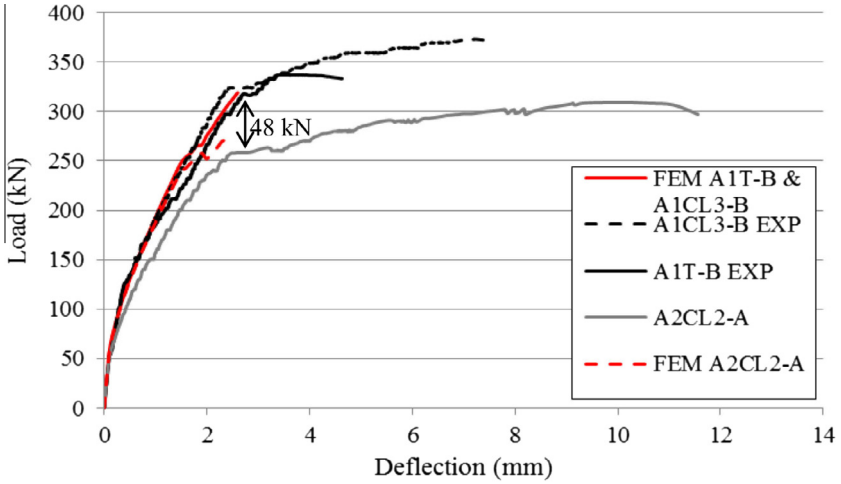

Fig. 15. Experimental and FE numerical model load–deflection curves for non-shear-repaired beams A1CL3-B, A2CL2-A and A1T-B.

strain value of the corroded steel bars. So, for this point, the steel corrosion did not lead to brittle failure of the steel bars either experimentally or in the numerical model, which is different from the behaviour of corroded RC beams in bending.

4.2. Load–deflection curves and failure modes for RC beams shear-repaired with NSM CFRP rods (A1CL3-SB and A1T-SB)

Fig. 18 shows the FE numerical load–deflection curves for both models created for beams repaired in shear with NSM and for the experimental beams. The results show good agreement among the behaviours of the four curves in terms of yielding capacity difference due to the corrosion found at the middle of the beam. This represented 12% of loss of cross section and led to 12% loss in yielding capacity, even though full convergence was not achieved for the two models due to the formation of new cracks and the simultaneous change of status of old cracks (i.e. reopening or reclosing of cracks).

The crack patterns of the FE numerical model were obtained for planes in three perpendicular directions. The *x*–*y* plane in Fig. 19 shows a large open crack (purple) occurring at the middle of the beam. The same effect of shear strengthening with NSM CFRP rods was captured in the FE numerical model. For non-shear repaired beam the model failed in a diagonal tension mode of failure with large shear cracks while, for the shear-repaired beam, the mode of failure changed to large flexural cracks at the middle of the beam as shown in Fig. 19.

For the crack patterns in the *x*–*z* and *y*–*z* planes shown in Fig. 20, some open cracks were observed at the middle and bottom of the beams while other open cracks were located at the bottom of the beams near the support.

The contribution to the shear strength of an RC beam provided by a system of NSM FRP strips was evaluated throughout the loading process by fulfilling the equilibrium, kinematic compatibility, and constitutive laws of both the materials composing the model and the bond between those materials [38,39]. Bianco et al. [20] proposed a predictive model to investigate the NSM shear strengthening contribution, and found that the contribution of the NSM laminates was limited by concrete tensile fracture along their available bond length. It was also found that the concrete around each NSM CFRP strip was not necessarily capable of carrying the stresses transferred to it, and could thus fracture in a

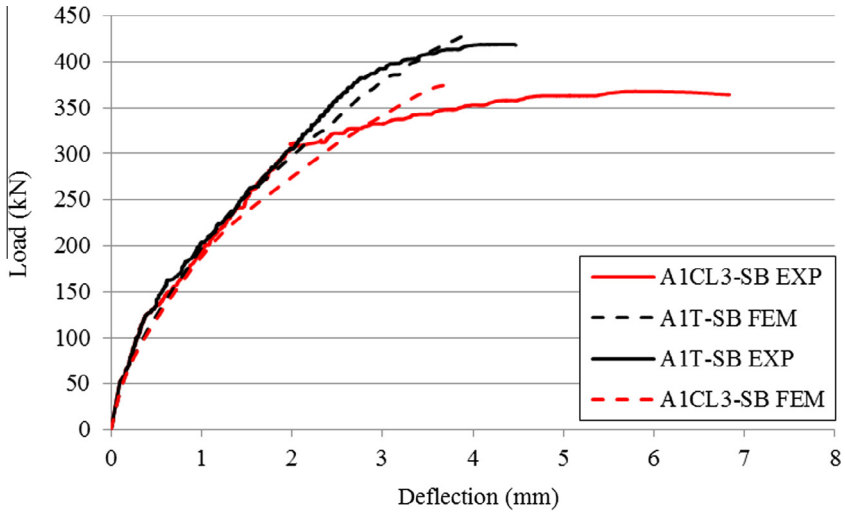

Fig. 18. Experimental and FE numerical model load–deflection curves for shear-repaired beams A1CL3-SB and A1T-SB.

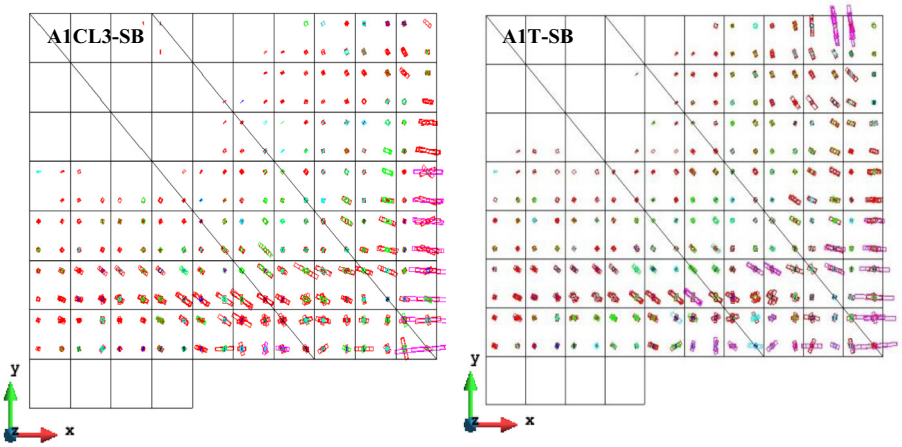

Fig. 19. FE crack patterns of the shear repaired beams in the *x*-*y* plane (in pink: crack completely open; in red: crack in the process of opening; in cyan: crack in the process of reopening; in green: crack in the process of closing; in blue: closed crack). (For interpretation of the references to color in this figure legend, the reader is referred to the web version of this article.)

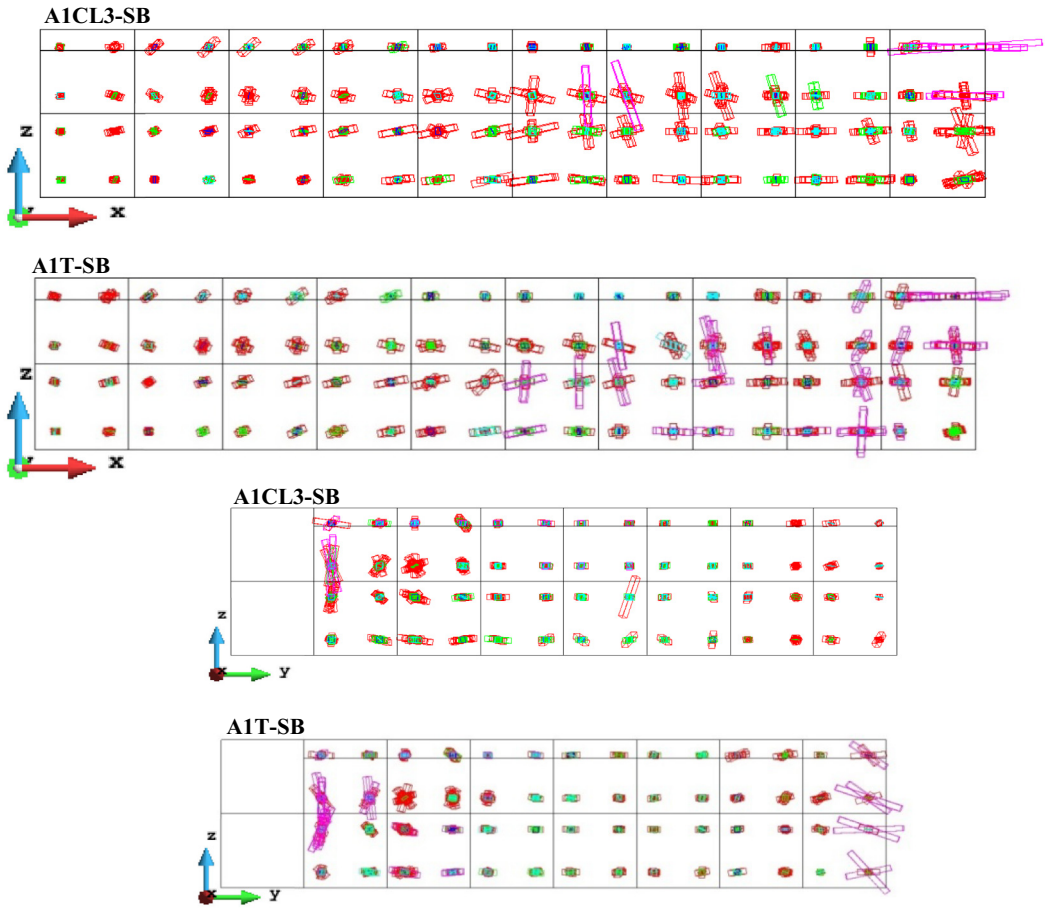

Fig. 20. FE crack patterns of the shear-repaired beams in *x–z* and *y–z* planes (in pink: crack completely open; in red: crack in the process of opening; in cyan: crack in the process of reopening; in green: crack in the process of closing; in blue: closed crack). (For interpretation of the references to color in this figure legend, the reader is referred to the web version of this article.)

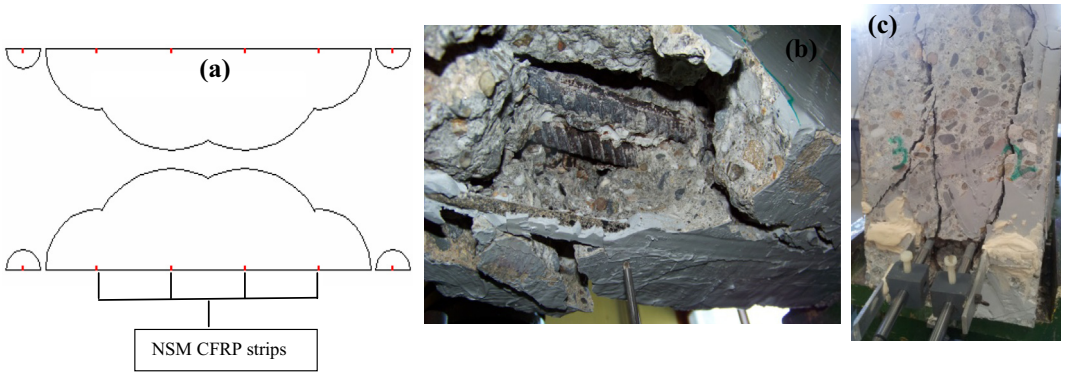

Fig. 21. (a) Section parallel to the crack plane for the theory of the failure mode proposed by Sena Cruz et al. [24]. (b) Splitting cracks at the bottom of the shear-repaired beams A1CL3-SB and A1T-SB. (c) Splitting cracks at the edge of the shear-repaired beams A1CL3-SB and A1T-SB.

semi-conical surface. If the laminate spacing was reduced, the semi-conical surfaces overlapped (shown in Fig. 21(a)), which allowed the interaction between laminates to be easily taken into account and the resulting concrete failure surface was almost parallel to the web face of the beam. The same crack patterns were found for the beams shear-repaired with NSM CFRP rods studied in this paper (A1T-SB and A1CL3-SB). At the bottom and the edge of the beams, there were visible splitting cracks (separation of the concrete sides including the NSM CFRP rods) which matched the predictive model proposed by Bianco et al. [20].

Fig. 21(a) shows a section parallel to the shear crack plane, presenting the semi-conical fracture surfaces of concrete due to excessive stresses of the approach proposed by Bianco et al. [20]. Fig. 21(b) and (c) presents the splitting cracks that occurred at the bottom and the edge of the shear-repaired beams A1T-SB and A1CL3-SB.

5. Conclusions

According to the results found in this paper, the following conclusions can be drawn:

1. The comparison between the FE numerical predictions and the experimental results showed a satisfactory level of accuracy of the proposed model in terms of capturing the load–deflection curves and the crack patterns.
2. The loss of cross section of steel bars was well captured by the FE numerical models, which reproduced the same reduction of the yielding capacity as found experimentally.
3. The effectiveness of the NSM technique was limited by the semi-conical effect of each NSM CFRP rod contribution and the non-repaired mid span point of the SB beams, which led to the appearance of splitting cracks at the middle of the RC beams strengthened in shear.
4. A FE numerical model taking account of both the interaction between the NSM CFRP rods and the concrete, and the bond-slip relationship between concrete and corroded steel bars is required in the future.

References

[1] Tayeh BA, Abu Bakar B, Megat Johari M, Voo YL. Mechanical and permeability properties of the interface between normal concrete substrate and ultra high performance fiber concrete overlay. Constr Build Mater 2012;36:538–48.
[2] Andrade C, Alonso C, Garcia D, Rodriguez J. Remaining lifetime of reinforced concrete structures: Effect of corrosion on the mechanical properties of the steel. In: International conference on life prediction of corrodible structures, NACE Cambridge, UK; 1991. p. 546–57.
[3] Al-Sulaimani G, Kaleemullah M, Basunbul I, Rasheeduzzafar. Influence of corrosion and cracking on bond behaviour and strength of reinforced concrete members. ACI Struct J 1990;87(2):220–31 (ASTM G1. 1990).
[4] Rodriguez J, Ortega L, Casal J. Load carrying capacity of concrete structures with corroded reinforcement. Constr Build Mater 1997;11(4):239–48.
[5] Chung L, Najm H, Balaguru P. Flexural behavior of concrete slabs with corroded bars. Cem Concr Compos 2008;30(3):184–93.
[6] Azad AK, Ahmad S, Azher SA. Residual strength of corrosion-damaged reinforced concrete beams. ACI Mater J 2007;104(1).
[7] Torres-Acosta AA, Navarro-Gutierrez S, Terán-Guillén J. Residual flexure capacity of corroded reinforced concrete beams. Eng Struct 2007;29(6):1145–52.
[8] Xia J, Jin W, Li L. Shear performance of reinforced concrete beams with corroded stirrups in chloride environment. Corros Sci 2011;53(5):1794–805.
[9] Wang X-H, Li B, Gao X-H, Liu X-L. Shear behaviour of RC beams with corrosion damaged partial length. Mater Struct 2012;45(3):351–79.
[10] Wang X-H, Gao X-H, Li B, Deng B-R. Effect of bond and corrosion within partial length on shear behaviour and load capacity of RC beam. Constr Build Mater 2011;25(4):1812–23.
[11] Zhu W, François R, Coronelli D, Cleland D. Effect of corrosion of reinforcement on the mechanical behaviour of highly corroded RC beams. Eng Struct 2013;56:544–54.
[12] Khan I, François R, Castel A. Experimental and analytical study of corroded shear-critical reinforced concrete beams. Mater Struct 2014:1–15.
[13] De Lorenzis L, Nanni A. Shear strengthening of reinforced concrete beams with near-surface mounted fiber-reinforced polymer rods. ACI Struct J 2001;98(1).
[14] Islam AA. Effects of NSM CFRP bars in shear strengthening of concrete members. ASCE; 2009. p. 1–14.
[15] Rizzo A, De Lorenzis L. Behavior and capacity of RC beams strengthened in shear with NSM FRP reinforcement. Constr Build Mater 2009;23(4):1555–67.
[16] Dias SJ, Barros JA. Performance of reinforced concrete T beams strengthened in shear with NSM CFRP laminates. Eng Struct 2010;32(2):373–84.
[17] Omran HY, El-Hacha R. Nonlinear 3D finite element modeling of RC beams strengthened with prestressed NSM-CFRP strips. Constr Build Mater 2012;31:74–85.
[18] Nanni A, Di Ludovico M, Parretti R. Shear strengthening of a PC bridge girder with NSM CFRP rectangular bars. Adv Struct Eng 2004;7(4):297–309.
[19] Barros JA, Baghi H, Dias SJ, Ventura-Gouveia A. A FEM-based model to predict the behaviour of RC beams shear strengthened according to the NSM technique. Eng Struct 2013;56:1192–206.
[20] Bianco V, Barros JA, Monti G. A new approach for modelling the NSM shear strengthening contribution in reinforced concrete beams. J Compos Constr 2010;14(1):36–48.
[21] Almassri B, Kreit A, Al Mahmoud F, Francois R. Behaviour of corroded shear-critical reinforced concrete beams repaired with NSM CFRP rods. Compos Struct 2015;123:204–15.
[22] Rots JG, De Borst R. Analysis of mixed-mode fracture in concrete. J Eng Mech 1987;113(11):1739–58.
[23] Suryanto B, Nagai K, Maekawa K. Modeling and analysis of shear-critical ECC members with anisotropic stress and strain fields. J Adv Concr Technol 2010;8(2):239–58.
[24] Sena Cruz JM, Barros JA, Gettu R, Azevedo ÁF. Bond behavior of near-surface mounted CFRP laminate strips under monotonic and cyclic loading. J Compos Constr 2006;10(4):295–303.
[25] Barros JAO, Baghi H, Dias SJE, Ventura-Gouveia A. A FEM-based model to predict the behaviour of RC beams shear strengthened according to the NSM technique. Eng Struct 2013;56:1192–206.
[26] Barros JA, Costa IG, Ventura-Gouveia A. CFRP flexural and shear strengthening technique for RC beams: experimental and numerical research. Adv Struct Eng 2011;14(3):551–71.
[27] Castel A, François R, Arliguie G. Mechanical behaviour of corroded reinforced concrete beams—Part 1: experimental study of corroded beams. Mater Struct 2000;33(9):539–44.
[28] Vidal T, Castel A, François R. Corrosion process and structural performance of a 17 year old reinforced concrete beam stored in chloride environment. Cem Concr Res 2007;37(11):1551–61.
[29] Kreit A, Al-Mahmoud F, Castel A, François R. Repairing corroded RC beam with near-surface mounted CFRP rods. Mater Struct 2011;44(7):1205–17.
[30] Almassri B, Kreit A, Mahmoud FA, François R. Mechanical behaviour of corroded RC beams strengthened by NSM CFRP rods. Compos Part B Eng 2014;64:97–107.
[31] Dang VH, François R, Coronelli D. Shear behaviour and load capacity of short reinforced concrete beams exposed to chloride environment. Eur J Environ Civ En 2015. http://dx.doi.org/10.1080/19648189.2015.1036129.
[32] François R, Khan I, Dang VH. Impact of corrosion on mechanical properties of steel embedded in 27-year-old corroded reinforced concrete beams. Mater Struct 2013;46(6):899–910.
[33] Zhu W, François R. Effect of corrosion pattern on the ductility of tensile reinforcement extracted from a 26-year-old corroded beam. Adv Concr Constr 2013;1(2):121–37.
[34] Apostolopoulos C, Papadakis V. Consequences of steel corrosion on the ductility properties of reinforcement bar. Constr Build Mater 2008;22(12):2316–24.
[35] Cairns J, Plizzari GA, Du Y, Law DW, Franzoni C. Mechanical properties of corrosion-damaged reinforcement. ACI Mater J 2005;102(4).
[36] Almusallam AA. Effect of degree of corrosion on the properties of reinforcing steel bars. Constr Build Mater 2001;15(8):361–8.
[37] Du Y, Clark L, Chan A. Residual capacity of corroded reinforcing bars. Mag Concr Res 2005;57(3):135–47.
[38] Bianco, V. Shear strengthening of RC beams by means of NSM FRP strips: Experimental evidence and analytical modeling [Ph.D. thesis]. Dept. of Structural Engrg. and Geotechnics, Sapienza Univ. of Rome, Italy; 2008.
[39] Bianco V, Barros JA, Monti G. Bond model of NSM-FRP strips in the context of the shear strengthening of RC beams. J Struct Eng 2009;135(6):619–31.